

## 1. SPIDER

The Segmented Planar Imaging Detector for Electro-Optical (EO) Reconnaissance (SPIDER) [1, 2] is a concept for an alternative EO imager that is lighter, smaller, cheaper and more power-efficient than state-of-the-art space telescopes. It is an optical interferometer that measures a total of 4440 visibilities (Fourier measurements)

$$\mathcal{V}(u, v) = \int_{-\infty}^{\infty} \int_{-\infty}^{\infty} I(l, m) e^{-2\pi i(lu + mv)} dl dm, \quad (1)$$

where the visibility  $\mathcal{V}$  measured at Fourier coordinate  $(u, v)$  is calculated using the sky-brightness  $I(l, m)$  at coordinates  $(l, m)$ .

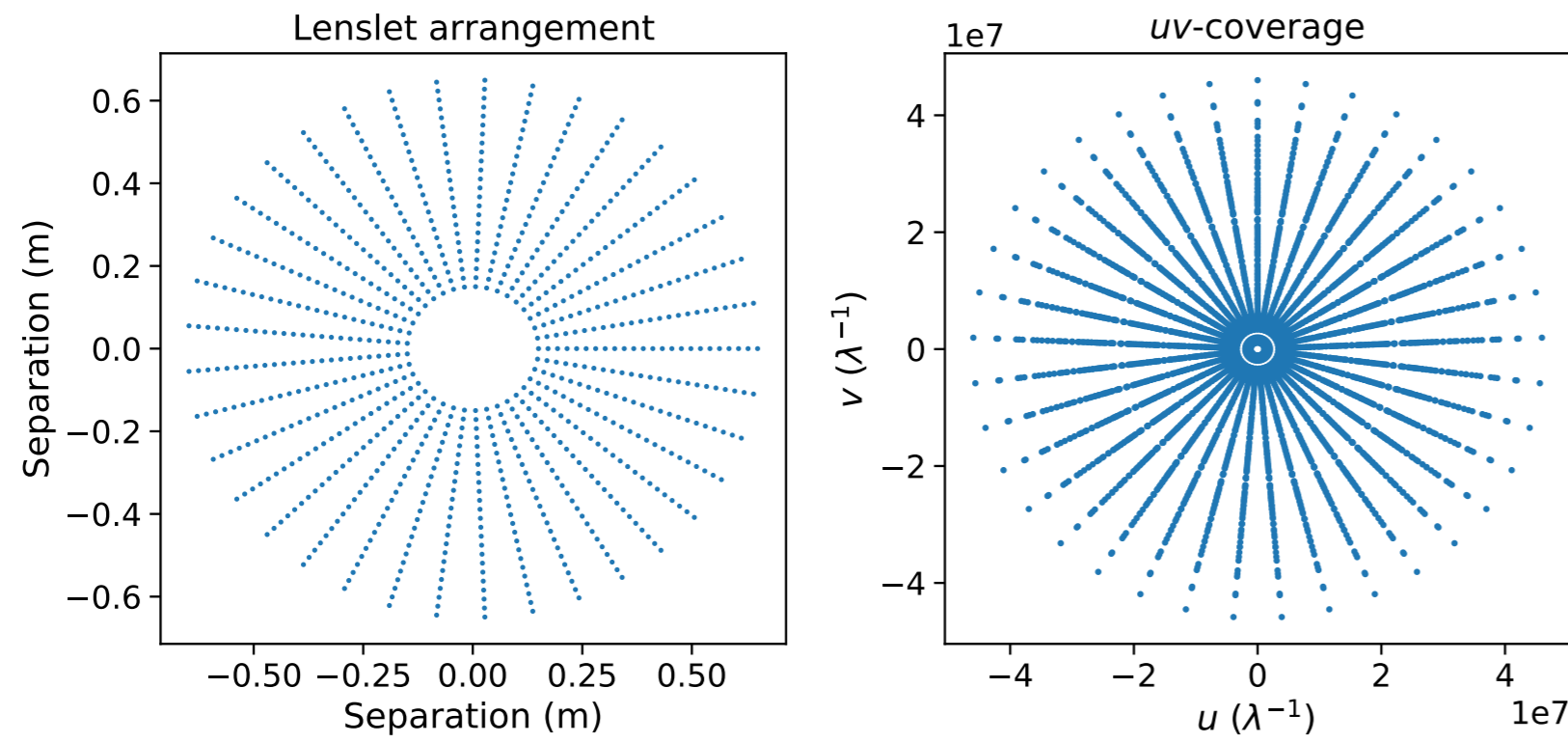


Figure: Arrangement of the lenslets of the SPIDER instrument (left) and the resulting Fourier sampling (right).

## 2. Interferometric Imaging Problem

The interferometric imaging problem can be concisely described as

$$\mathbf{y} = \Phi \mathbf{x} + \mathbf{n}, \quad (2)$$

with Fourier measurements  $\mathbf{y} \in \mathbb{C}^K$ , image  $\mathbf{x} \in \mathbb{R}^N$ , measurement noise  $\mathbf{n} \in \mathbb{C}^K$ , and measurement operator  $\Phi: \mathbb{R}^N \rightarrow \mathbb{C}^K$ , which is a Fourier transform mapping from an image with  $N$  pixels to  $K$  non-uniform Fourier measurements.

For our particular implementation we have  $K = 4440$  non-uniform measurements,  $N = 256 \times 256$  pixels, and the measurement operator is modelled using a non-uniform fast Fourier transform (NUFFT) [3].

We can find an approximation to  $\mathbf{x}$  by solving the minimization problem

$$\mathbf{x}^* = \arg \min_{\mathbf{x} \in X} \|\Phi \mathbf{x} - \mathbf{y}\|_{\ell_2}^2 + \lambda \|\Psi^T \mathbf{x}\|_{\ell_1}, \quad (3)$$

with  $\lambda$  the regularization parameter and  $\Psi$  a dictionary of bases in which the true signal is naturally sparse. E.g. Pratley et al. 2018 [4] use convex optimization algorithms with a dictionary of wavelet bases to reconstruct images in radio interferometry.

These reconstruction techniques are limited by the information captured in handcrafted priors and are computationally expensive because they evaluate the measurement operator every iteration.

## 4. Experiment

Simulated measurements are generated following Equation 2, adding Gaussian measurement noise with an input-signal-to-noise ratio (ISNR) of 30dB

$$\sigma = \frac{\|\Phi \mathbf{x}\|_{\ell_2}}{\sqrt{K}} \cdot 10^{-\frac{\text{ISNR}}{20}}. \quad (6)$$

The U-Net and GU-Net are trained using 2000,  $256 \times 256$  natural images from the COCO dataset [8].

Networks are first trained for 200 epochs on the ADAM optimizer, a learning rate of 0.001, and a batch size of 5.

Using transfer learning, we repurpose the network to reconstruct images in domains with lower availability of data. We train the networks for 100 epochs on 300 images and evaluate on 150 images from the datasets:

- Galaxy simulations from [IllustrisTNG simulations](#) [9]
- Satellite images from [Deep Globe satellite challenge](#) [10]

## 5. Results

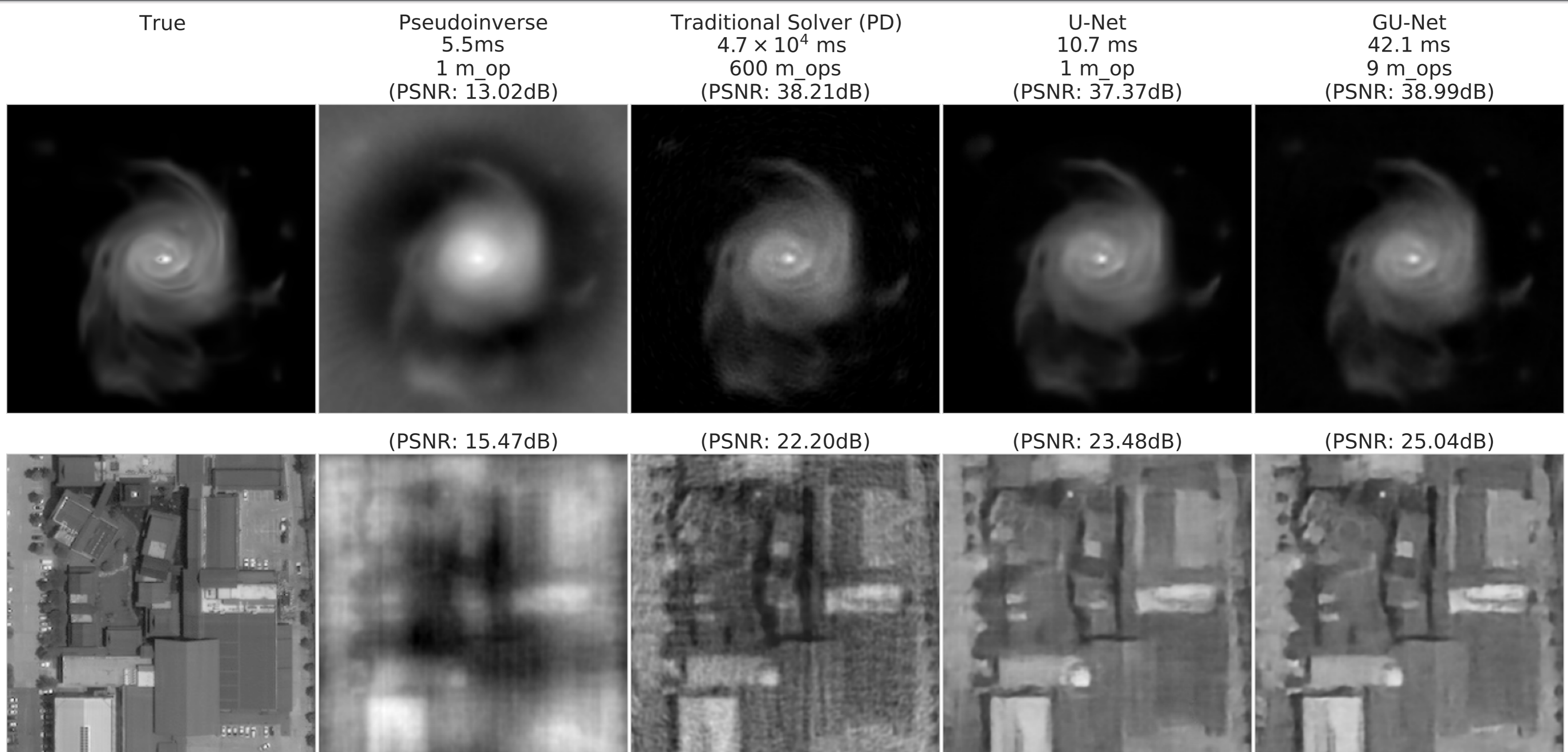


Figure: Reconstructions and the computation time, number of (full-scale) measurement operator evaluations (m\_ops), and peak signal-to-noise ratio (PSNR) of the reconstructions.

## 3. Learned Interferometric Imaging [5]

We leverage learned imaging techniques to construct models with data-driven priors and lower computational cost by evaluating the measurement operator sparingly.

Learned postprocessing methods learn a network to correct for artefacts introduced by applying the pseudoinverse of the measurement operator to the measurements

$$\hat{\mathbf{x}} = \Phi_0^\dagger \mathbf{y} = \Lambda_\theta \Phi^\dagger \mathbf{y}, \quad (4)$$

with  $\Lambda_\theta$  the learned denoising network, and  $\Phi^\dagger$  the pseudoinverse of the measurement operator. We use a U-Net [6] architecture for our learned postprocessing network.

Unrolled iterative approaches combine learned networks with information captured by the measurement operator, mimicking traditional solving approaches. They learn data-driven priors and need less iterations (and therefore computation) to converge to a solution.

To apply the measurement operator at different resolution scales in the network, we define sub-scale measurement operators,  $\Phi_i: \mathbb{R}^{N_i} \rightarrow \mathbb{C}^{K_i}$ , working on a reduced image resolution  $N_i \leq N$ , and a restricted Fourier measurement space,  $K_i \leq K$ , by applying low-pass filters to the Fourier coefficients (cf. [7]).

We integrate measurement information on all scales in the U-Net structure by including a (filtered) gradient of the data fidelity functional, as well as a restricted reconstruction using the adjoint of the (sub-scale) measurement operator

$$\tilde{\mathbf{x}}_i = \Lambda_{i,\theta}(\mathbf{x}_i, \nabla_{\mathbf{x}_i} \mathcal{L}(\Phi_i \mathbf{x}_i, \mathbf{y}_i), \nabla_{\mathbf{x}_i}^T \mathcal{L}(\Phi_i \mathbf{x}_i, \mathbf{y}_i), \Phi_i^* \mathbf{y}_i). \quad (5)$$

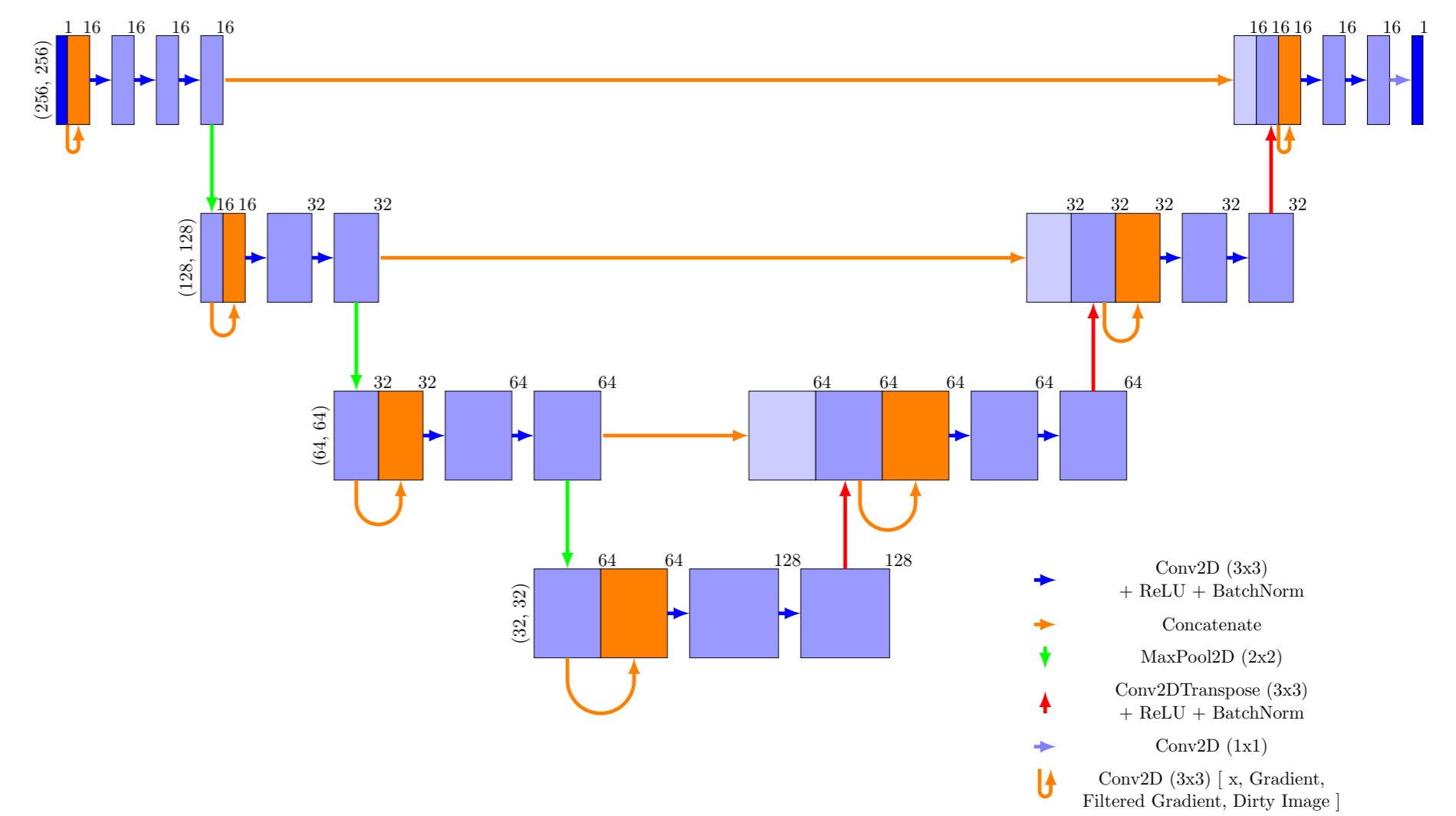


Figure: GU-Net architecture

## References

- [1] Kendrick et al. 2013, "Segmented Planar Imaging Detector for EO Reconnaissance"
- [2] Duncan et al. 2015, "SPIDER: Next generation chip scale imaging sensor"
- [3] Dutt & Rohklin 1993, "Fast Fourier Transforms for Nonequispaced Data"
- [4] Pratley et al. 2018, "Robust Sparse Image Reconstruction of Radio Interferometric Observations with Purify"
- [5] Mars et al. 2023, "Learned Interferometric Imaging for the SPIDER Instrument"
- [6] Ronneberger et al. 2015, "U-Net: Convolutional Networks for Biomedical Image Segmentation"
- [7] Pan & Betcke 2022, "On Learning the Invisible in Photoacoustic Tomography with Flat Directionally Sensitive Detector"
- [8] Lin et al. 2014, "Microsoft COCO: Common Objects in Context"
- [9] Nelson et al. 2019, "The IllustrisTNG Simulations: Public Data Release"
- [10] Demir et al. 2018, "DeepGlobe 2018: A Challenge to Parse the Earth through Satellite Images"